water

MDPI

Article

Long-Term (2007–2024) Thermal and Water Quality Dynamics in Lake Tisza (Kisköre Reservoir), Hungary: A Shallow Freshwater Ecosystem Under Climate Pressure

David Matamoros [1], György Szabó [1], Eduárd Csépes [2], Borbála Benkhard [1], Emőke Kiss [1], Mária Vasvári [1], Péter Csorba [1] and Tamás Mester [1,*]

[1] Department of Landscape Protection and Environmental Geography, Institute of Earth Science, Faculty of Science and Technology, University of Debrecen, 4032 Debrecen, Hungary; nicolas.matamoros@science.unideb.hu (D.M.); szabo.gyorgy@science.unideb.hu (G.S.); benkhard.borbala@science.unideb.hu (B.B.); kiss.emoke@science.unideb.hu (E.K.); vasvari.maria@science.unideb.hu (M.V.); csorba.peter@science.unideb.hu (P.C.)

[2] Regional Laboratory of the Middle-Tisza District Water Directorate, Tiszaliget 9688/3, 5000 Szolnok, Hungary; csepese@kotivizig.hu

* Correspondence: mester.tamas@science.unideb.hu

Abstract

Freshwater shallow lakes are vulnerable to global warming, putting entire aquatic ecosystems at risk, but evidence from managed reservoirs remains limited despite the existence of long-term empirical data. Using data from 29 stations on Lake Tisza covering an 18-year period (2007–2024), this study quantifies warming rates, thermal stress patterns and trends in water quality in lacustrine, transitional and riverine zones. Lake areas warmed at a rate of 0.90 °C/decade ($p < 0.001$), faster than the river/transition areas and even than global averages in shallow lakes. Temperature-critical years now affect 90.4% of lake stations, compared with 59.6% in 2007–2012. A strong negative correlation between temperature and dissolved oxygen was observed along all systems (Spearman's p; river: −0.83, transition: −0.65, lake: −0.53), indicating thermal-driven deoxygenation risk. At the same time, a water quality index (conductivity, pH, BOD_5, total nitrogen and phosphorus, total coliforms) showed an improvement (lake WQI: 63.7 to 74.3). Principal component analysis explained 85% of its variance, showing spatial gradients of eutrophication and fecal contamination, with lacustrine homogenization suggesting management interventions. Lake Tisza is warming faster than global shallow lake averages, with critical implications for the ecosystem's function; nonetheless, the coexistence of thermal deterioration with improvements in its WQI reveals the effectiveness of the intermittent discharge system and the need for climate-adapted monitoring frameworks that incorporate thermal vulnerability into water quality assessment for regulated shallow lakes under climate change pressure.

Keywords: water quality; freshwater warming; temperature trend; spatiotemporal variability; thermal stress; reservoir management

Check for updates

Academic Editor: Ryszard Gołdyn

Received: 25 March 2026
Revised: 26 May 2026
Accepted: 31 May 2026
Published: 3 June 2026

Copyright: © 2026 by the authors. Licensee MDPI, Basel, Switzerland. This article is an open access article distributed under the terms and conditions of the Creative Commons Attribution (CC BY) license.

1. Introduction

Freshwater ecosystems are among the most vulnerable and threatened systems on the planet [1]. The advance of the industrial era has led to their progressive deterioration, transforming their characteristics and functioning [2]. Preserving them has become increasingly important due to their ecosystem, tourism and economic value [3]. In recent

decades, climate change has been an additional driver of instability, with altered hydrological regimes intensified by rising temperatures, leading to changes in water column processes, eutrophication, cyanobacterial blooms and reduced ecological quality [1–4]. The structure of these systems is being altered day by day by extreme hydrological changes and shifts in seasonal patterns, with repercussions for water security and public health for local and regional economies [5,6].

However, thermal forcing, resulting from irresponsible environmental management, has caused many lakes to warm rapidly, although the rate and direction of change vary regionally due to climate and local characteristics such as depth and transparency [6]. Global studies have demonstrated widespread warming of surface waters, with an average rate of 0.34 °C/decade between 1985 and 2009 [7]. This warming reinforces thermal stratification and alters seasonal mixing regimes, a phenomenon that global models indicate is already occurring and is projected to intensify [8]. Since mixing governs oxygen replenishment and nutrient redistribution, changes in stratification quickly impact water quality, resulting in widespread deoxygenation in temperate lakes due to lower oxygen solubility in warmer water and stronger stratification, which reduces ventilation [9]. In parallel, there is a strong link between climate and eutrophication/harmful algal blooms (HABs). A long-standing hypothesis holds that warming acts as a catalyst that favors cyanobacteria [10]. However, an influential line of work emphasizes that HABs are primarily driven by nutrients, and that climate change amplifies them, creating a "climate penalty" that requires more ambitious nutrient reductions [11].

Climate change also alters water quality through increased dissolved organic carbon (DOC) or "browning". Complementary explanations point to the recovery from historical acid deposition [12] and, in more recent analyses, to climatic factors that are displacing deposition as the dominant control in many regions [13]. For river-connected systems, hydrological variability is another critical link, and ecological risk tends to increase with the magnitude of flow disturbance [14]. In reservoir systems the interaction between the operated hydrological regime (filling/emptying) and climate forcing creates complex interactions and dynamics that require specific analysis [15]. This framework aligns with policies such as the EU Water Framework Directive, which requires the achievement of "good" ecological status [16].

There are similar cases where warming patterns are accelerating in other reservoirs, such as in the case of 35 Czech lakes, which increased by an average of 0.59 °C/decade over 31 years of study, presenting as different involving factors either seasonal or morphometric interactions [17]. In addition, a different behavior is expected in lake thermal regions, which will become warmer, thus drastically reducing the number of cold-water lakes in the north [18]. In all these respects, efforts to model these behaviors, which are less anomalous over time, highlight the need for tools to predict these changes [19]. Therefore, the planning of a complex system due to the multiple ecotones lying in the Tisza Lake reservoir recognizes the coupled relevance of water quantity and quality in a changing climate [15]. Long-term observations in Hungary show notable signs of warming in the Tisza River [20], where hydro-chemical assessments highlight the role of hydrological operation and fill/drain cycles in shaping water quality patterns [3].

Despite these advances, three critical knowledge gaps persist that are particularly relevant for shallow regulated reservoirs. First, most long-term studies focus on natural lakes where the dynamics differ substantially from shallow systems; a few studies addressing shallow managed reservoirs report highly variable warming rates but lack the multi-station, multi-decadal resolution needed to characterize intra-reservoir spatial gradients. Second, while the temperature and dissolved oxygen relationship is well established in controlled conditions, its expression across the lotic-to-lentic gradient remains continuous, where

flow velocity, residence time, and progressive biochemical oxygen demand shift remain poorly documented in field-based long-term datasets. Third, the simultaneous assessment of thermal stress trajectories and conventional water quality indices (WQIs) in the same system over time is rare due to management interventions that improve chemical quality but may mask or amplify thermal vulnerability, which standard monitoring frameworks fail to detect.

This study addresses key gaps using an 18-year dataset (2007–2024) from Lake Tisza, guided by three central questions: (Q1) Is the lake warming faster than global and regional benchmarks for shallow lakes, and does this rate vary along its lotic-to-lentic gradient? (Q2) Does thermal intensification increase ecophysiological stress and dissolved oxygen depletion risk? (Q3) Are thermal trends and conventional water quality indicators coupled or dissociated, and what does this imply for current management under climate warming? To answer these questions, five objectives are pursued: (1) to quantify spatiotemporal water temperature evolution; (2) to classify thermal stress (optimal, suboptimal, critical) using ecophysiological thresholds; (3) to evaluate temperature–dissolved oxygen dynamics; (4) to assess trends in conductivity, pH, BOD_5, total nitrogen, phosphorus, and coliforms; and (5) to identify spatial patterns via PCA and hierarchical clustering. The aim is to test whether thermal deterioration and water quality indicators are dissociated, thus evaluating the management effectiveness of current management strategies in the face of the system's progressive warming.

2. Materials and Methods

2.1. Description of the Study Area

Lake Tisza, located in the Great Hungarian Plain, has been classified as the second largest body of water in Hungary and its largest reservoir (127 km^2), with an average depth of 1.45 m. Its modern formation in 1967 responded to water management objectives: energy support, irrigation and flood control. Its current irregular morphology is the result of embankment and infrastructure consolidation in the Tisza River valley, an area that was historically a dynamic "land of wild waters" [3].

Its water regime is characterized by four main sub-basins (Tiszavalk, Poroszló, Sarud, Abádszalók), which have significant gradients in circulation, water quality, and ecological functioning, requiring a structured spatial analysis [21].

However, this study maintains a specific evaluation for each monitoring point structured in 29 georeferenced stations [HD72/EOV (EPSG: 23700)] to capture longitudinal and transverse variability, including areas of riverine, transitional, and lacustrine influence in an 18-year time series (2007–2024). GIS mapping (QGIS 3.34) integrated the lake boundary, water network, and sub-basins to document spatial representativeness and facilitate further analysis (Figure 1).

2.2. Water Sampling

In accordance with the European Union Water Framework Directive (WFD), monthly monitoring was carried out during the period 2007–2024 by the Middle Tisza District Water Directorate in conjunction with the laboratory where they operate and process samples following national standards and guidelines at monthly intervals throughout every year.

Sampling was conducted in accordance with MSZ ISO 5667-4:2017. At each site, surface-water samples were collected from a boat from the upper 0–20 cm of the water column. Temperature, pH, electrical conductivity (EC) and dissolved oxygen (DO) were measured in situ within the same surface layer using a HACH® HQ40d multiparameter (Hach Company, Loveland, CO, USA), Hydro-chemical parameters were determined in the laboratory following the corresponding standards: BOD_5 (MSZ EN 1899-1:2000; MSZ EN

1899-2:2000), Total N (MSZ 448-27:1985), Total P (MSZ 260-20:1980), and Total Coliforms (MSZ EN ISO 9308-1).

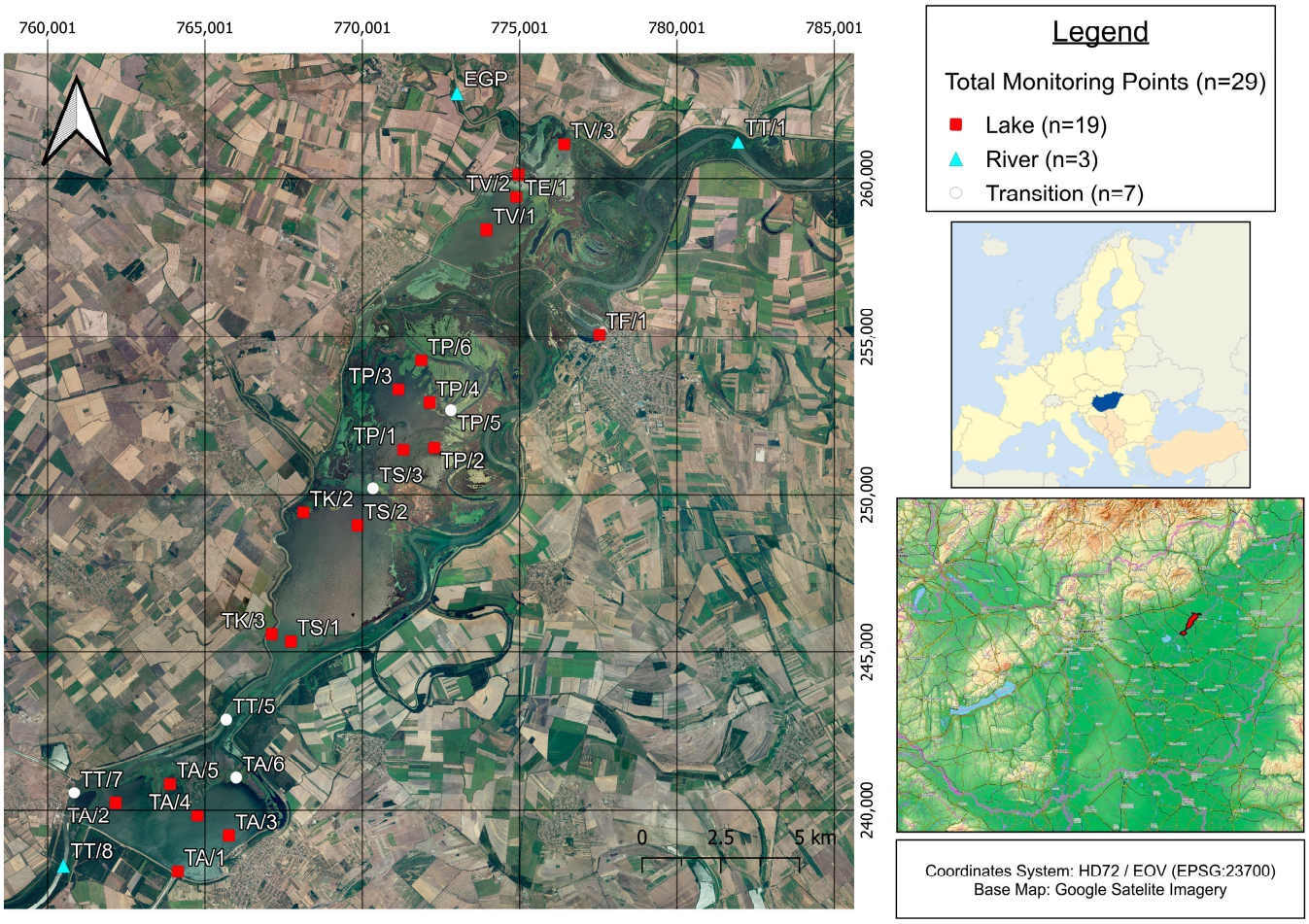


Figure 1. Spatial distribution of monitoring points classified according to their hydrological regime (lake/river/transition).

The monitoring stations have been classified into three types of water bodies—riverine, transitional, and lacustrine—according to their position along the lotic–lentic gradient of the reservoir and their hydraulic connectivity with the main river channel (Figure 1). The river stations (EGP, TT/1, TT/8) were located within the main river channel, dominated by direct flow. The transitional stations (TP/7, TP/5, TS/3, TK/1, TT/5, TT/7, TA/6) occupied channel-basin interfaces and connecting sections, characterized by flow deceleration and intensified mixing processes. The lake stations (TV/1-3, TE/1, TF/1, TP/1-4, TP/6, TS/1-2, TK/2-3, TA/1-5) were in open water sub-basins, where advective influence is minimal and vertical mixing processes predominate.

2.3. Evaluation Criteria for Each Hydrological Regime

The quality thresholds for physicochemical parameters (conductivity, BOD_5, total N and P) are based on the official limit values in Hungary, established by Decree 10/2010 (VIII.18.) VM to implement the Water Framework Directive (2000/60/EC) cited in Tables 1 and 2. These values, defined by water body type, were operationally grouped into three hydraulic categories: “River”, “Transition” and “Lake”, to align the assessment with the natural hydrodynamic zoning of Lake Tisza, a transitional system with a lotic–lentic gradient. However, it is important to emphasize that for the coliform parameter, the same limits were adopted as for sanitary and recreational control criteria. Although it is not a

central indicator for the ecological diagnosis of the WFD, it functions as a sentinel indicator of fecal contamination and anthropogenic pressure. In a shallow, multi-use system such as Lake Tisza (recreation, settlements, agriculture), this parameter allows for the tracking of diffuse wastewater inflow and the assessment of hygienic-sanitary risk, thus complementing the analysis of eutrophication.

Table 1. Quality thresholds for physicochemical-microbiological parameters in the Water Framework Directive (2000/60/EC) for "River", "Transition", and "Lake.".

Parameter	Type	Unit	Optimal	Sub-Optimal	Critical
Conductivity	River	µS/cm	<900	900–1200	>1200
	Transition	µS/cm	<900	900–1200	>1200
	Lake	µS/cm	<900	900–1200	>1200
BOD [5]	River	mg/L	<3	3–6	>6
	Transition	mg/L	<3	3–6	>6
	Lake	mg/L	<3	3–6	>6
Total N	River	mg/L	<1.0	1.0–3.0	>3.0
	Transition	mg/L	<0.6	0.6–2.0	>2.0
	Lake	mg/L	<0.4	0.4–1.5	>1.5
Total P	River	mg/L	<0.05	0.05–0.20	>0.20
	Transition	mg/L	<0.05	0.05–0.15	>0.15
	Lake	mg/L	<0.03	0.03–0.05	>0.05
Total Coliforms	River	UFC/100 mL	<500	500–10,000	>10,000
	Transition	UFC/100 mL	<500	500–10,000	>10,000
	Lake	UFC/100 mL	<500	500–10,000	>10,000
pH	River	-	6.5–8.5	6.0–6.5//8.5–9.0	<6.0//>9.0
	Transition	-	6.5–8.5	6.0–6.5//8.5–9.0	<6.0//>9.0
	Lake	-	6.5–8.5	6.0–6.5//8.5–9.0	<6.0//>9.0

Table 2. Operational classification scheme for dissolved oxygen and temperature grouped by hydraulic type.

Parameter	Category	Unit	Water Body		
			River	Transition	Lake (Epilimnion)
Dissolved Oxygen	1. Critical	mg/L	<3.0	<3.0	<3.0
	2. Lower Suboptimal	mg/L	3.0–5.0	3.0–5.0	3.0–5.0
	3. Optimal/acceptable oxygenation	mg/L	5.0–9.0	5.0–9.0	5.0–9.0
		%Sat	61–110	61–110	61–110
	4. Upper Suboptimal	%Sat	>110–150	>110–150	>110–150
	5. Upper Critical	%Sat	>150	>150	>150
Temperature	1. Critical Thermal Minimum	°C	0–2	0- 3	0–2
	2. Low Incipient Temperature	°C	2–5	3–7	2–5
	3. Lower Suboptimal Range	°C	5–10	7–12	5–8
	4. Optimal Range	°C	10–18	12–20	8–18

Table 2. *Cont.*

Parameter	Category	Unit	Water Body		
			River	Transition	Lake (Epilimnion)
Temperature	5. Upper Suboptimal Range	°C	18–22	20–24	18–22
	6. High Incipient Temperature	°C	22–25	24–27	22–25
	7. Critical Thermal Maximum	°C	>25	>27	>25

The thermal classification applied across three categories (critical–suboptimal–optimal) aims to evaluate limnological functioning in lotic–lentic regimes, considering biological processes, functional ranges, and mortality risks for aquatic organisms, in accordance with the WFD, which considers thermal conditions as a physical–chemical element that supports ecological status. The river–transition–lake criterion adopted captures the fundamental differences in hydrodynamic and limnological processes in longitudinal gradients typical of reservoirs such as the Tisza, where there are fluctuations in flow velocity, residence time, transparency, and biogeochemical dynamics that justify the thermal ranges established in Table 3 [22,23].

Table 3. CB-WQI classification.

Canadian Council of Ministers of the Environment Water Quality Index	
80–100	Excellent Water Quality
60–80	Good Water Quality
40–60	Fair Water Quality
20–40	Marginal Water Quality
0–20	Poor Water Quality

A classification of dissolved oxygen and its saturation (critical–suboptimal–optimal–supersaturated) was established in line with the WFD. The "optimal" ranges were based on Hungarian regulations for surface waters [24], while the "critical" ranges were defined using agreed ecophysiological thresholds: <3 mg/L indicates lethal hypoxia and >110–120% saturation indicates eutrophication. Separate categories were applied for river, transition, and lake areas to reflect the hydraulic differences (mixing, residence, stratification) that control oxygen dynamics [25].

2.4. Statistical Analysis and Spatial Analysis

All statistical analyses were performed using Rstudio 2024.12.0 + 467. A complete description of each method, including all formulas, assumptions, and validation tests, is provided in Supplementary Materials S1.

The heat map was created using averages for each period from 2007–2012, 2013–2018, 2019–2024, distributed homogeneously by month, site, and water regime. R packages such as ggplot, dplyr, stats and tidyr were used to filter the months of interest, group by site (s), month (m), period (p), and water body, and calculate the average for subsequent color-coded representation indicating higher or lower temperatures allowing seasonal comparisons by the following formula:

$$\overline{T} = \frac{1}{n}\sum_{k=1}^{n} T \quad (1)$$

where the average temperature from the same monitoring site, month and period its determined by the sum of all temperatures (n) divided by the number of measurements (T). For each monitoring site, the annual average temperature was calculated for all observations, and then the annual values were averaged by hydrological regime (lake–transition–river), observing multi-line time series.

The proportion of years classified as thermally critical was calculated for each period and water body type.

To determine the percentage of each type of water body that falls within classification type (1–7) (Table 2), the temporal evolution of critical thermal conditions was evaluated using the proportion of annual observations in the periods (2007–2012, 2013–2018, 2019–2024) by the expression:

$$\%Critical_{w,p} = 100.\frac{\sum I_{i,t}}{N_{w,p}} \quad (2)$$

This expression counts the years that were critical by group, divided by the total number of observations expressed as a percentage, referring to $I_{i,t}$ if the observation falls under critical values of either 1 or 0 from Table 2, and $N_{w,p}$ is the total number of observations by period and water body.

Linear regression was applied to annual mean temperatures at each monitoring site to estimate warming rates. A positive slope indicates warming, negative indicates cooling. Trends are expressed as °C/decade.

The average for each point was calculated annually and then grouped by type (river, transition, lake) using a linear regression model to evaluate the trend, where $T_i(t)$ denotes the annual summer temperature metric at site, $\beta_{0,i}$ is the intercept, $\beta_{1,i}$ is the slope and the residual error is $\varepsilon_{i,t}$:

$$T_i(t) = \beta_{0,i} + \beta_{1,i}t + \varepsilon_{i,t} \quad (3)$$

where β_1 reflects the average change in °C/year = °C/decade, $\bar{t}$ means the year's average, $T_i(t)$ is temperature by site/year, and $\overline{T}_i$ is mean temperature by site throughout the series corresponding to expression ($\beta_{1,i}$) [26]:

$$\beta_{1,i} = \frac{\sum_t (t - \bar{t})[T_i(t) - \overline{T}_i]}{\sum_t (t - \bar{t})^2} \quad (4)$$

Which is interpreted as an increase, decrease, or no clear trend under the following criteria:

$$\beta_{1,i} < 0\ ;\ Cooling$$
$$\beta_{1,i} > 0\ ;\ Heating$$
$$\beta_{1,i} = 0\ ;\ No\ clear\ trend$$

For each water body type, the boxplot displays: median (central line): 50th percentile, interquartile range (IQR = Q3 − Q1): box limits (25th to 75th percentile), whiskers: extend to Q1 − 1.5 × IQR and Q3 + 1.5 × IQR, points beyond whiskers: potential outliers.

The distribution of water temperature among the types of water regimes for the period 2007–2024 was analyzed by grouping temperatures by type in conjunction with the violin method, which represents the density of observations, in addition to calculating the median, interquartile range, and extreme values, whose logic is IQR = Q3 − Q1, with its lower limit = Q1 − 1.5 × IQR and upper limit = Q3 + 1.5 × IQR.

For each monitoring site, trends for minimum, maximum, and mean temperatures were calculated and expressed as °C/decade following the linear model in Section S1.4 in the Supplementary Materials.

For each site in the river (3 monitoring points), lake (19 monitoring points), and transition zone (7 monitoring points), and for temperature variations classified as mini-

mum, maximum, and average, their series were calculated by adjusting them to a straight line over time using Equation (3) for the 3 temperature variations and expressing them in °C/decade using:

$$Trend_i = 10x\beta_{1,i} \quad (5)$$

Spearman's rank correlation coefficient with 95% confidence intervals was used to assess the monotonic relationship between temperature and dissolved oxygen. A linear model was fitted to visualize the relationship.

The correlation between temperature ranges and dissolved oxygen using Spearman's correlation coefficient with 95% confidence intervals was calculated using:

$$\rho = 1 - \frac{6\sum d_i^2}{n(n^2-1)} \quad (6)$$

The difference between the ranges of both variables d_i and their number of observations (n) used to quantify their monotonic relationship was determined, while adjusting a straight line that corresponds to:

$$DO_i = \alpha + \beta(T^\circ)_i + \varepsilon_i \quad (7)$$

PCA was performed on standardized variables to identify spatial gradients. Hierarchical clustering using Ward's method with Euclidean distance grouped monitoring sites with similar environmental characteristics.

Due to the nature of the variables and their different units of measurement, standardization was carried out for the different periods knowing the original variable value (x_{ij}), mean ($\overline{x}_j$), and (s_j) standard deviation, extracting their main components and summarizing them into two axes to analyze the degree of similarity between the variables:

$$z_{ij} = \frac{x_{ij} - \overline{x}_j}{s_j} \quad (8)$$

Moreover, a hierarchical clustering analysis was performed on period G1 (2007–2012), G2 (2013–2018), G3 (2019–2024) to identify groups of monitoring sites that had similar environmental characteristics. Prior to clustering, the variables were standardized to a mean of zero and a variance of one. Dissimilarity among sites was quantified using Euclidean distance, and clusters were generated using Ward's minimum variance method. Then, the dendrogram was cut at a selected height to define the main site groups.

The Canadian Border Water Quality Index (CB-WQI) was calculated to synthesize six parameters (conductivity, pH, BOD_5, total N, total P, total coliforms). Parameter values were scored as optimal (100), suboptimal (60), or critical (20) based on thresholds from Table 1. The final WQI is the arithmetic mean of parameter score defined by regulations/criteria for each type of water body, categorizing them (100, 60, 20) corresponding to a design decision [27,28] based on [29] in Table 3:

$$C_{i,p} = \left\{ \begin{array}{c} Optimal[100]\ ;\ X_{i,p} \le L_{p,opt} \\ Suboptimal[60]\ ;\ L_{p,\,opt} < X_{i,\,p} \le L_{p,\,sub} \\ Critical[20]\ ;\ X_{i,p} > L_{p,sub} \end{array} \right\} \quad (9)$$

$$CB - WQI_i = \frac{1}{n_i}\sum_{p=i}^{n_i} S.I_{i,p} \quad (10)$$

The rate of missing data was highest during the winter months, at 7.2%, and lowest in the summer, at 3.1%; overall, missing data accounted for 4.7% (523 out of 11,136) of the total. Since this percentage is less than 5%, according to [30] listwise deletion was applied

for univariate analyses and pairwise deletion was applied for multivariate analyses. No imputation was performed in order to avoid introducing bias into the dataset. Instead, water quality parameters were aggregated into three multi-annual periods (2007–2012, 2013–2018, 2019–2024), allowing the use of available observations while reducing the impact of data gaps. The water quality index (WQI) was calculated as the average of parameter-specific subindices, considering only available parameters for each site and period.

2.5. Spatial Analysis in QGIS 3.34

Inverse Distance Weighting (IDW) with power parameter $p = 2$ was applied to generate continuous temperature and dissolved oxygen surfaces from the 29 monitoring points.

The average temperature was calculated for each site for the months from June to September, using the Inverse Distance Weighting (IDW) method for either temperature or dissolved oxygen with the following equation:

$$w_i = \frac{1}{d_i^p} \tag{11}$$

where (di) represents the distance between the monitoring site x and the interpolated point and p is the weight parameter (normally 2). Ti is the measured temperature and T(x) is the expected temperature:

$$T(x) = \frac{\sum_{i=1} w_i T_i}{\sum_{i=1} w_i} \tag{12}$$

To generate continuous temperature surfaces across the river–transition–lake, a classified color gradient was used to visualize spatial patterns or, in the dissolved oxygen case, to show the anoxic conditions presented.

3. Results

3.1. Spatiotemporal Temperature Variability in the Water Regime

To determine seasonal temperature variability between summer periods, the average was maintained by a combination of site, month, category, and period, and simultaneous comparison of seasonal patterns whose differences highlight an intensification of tones in the period (2019–2024), reaching maximum values of (25–27.5) °C in the lake sector (Figure 2).

Complementary to the heat map, significant interannual variability toward colder winters and warmer summers is confirmed, clarifying that warm episodes comprehensively affect the system by type, whether lake, transition, or river, with higher average values throughout the chronology (Figure 3).

For a better understanding of the thermal distribution across the lake, a descriptive spatial analysis of monthly averages (June–September) for the period 2007–2024 has been prepared, showing progressive warming and persistent thermal zones (Figure 4). In addition, as Supplementary Information, Figure 5 establishes the water temperature index for each station, including multi-year winter–summer temperatures, following the classification in Table 2 for temperature. The heterogeneity reflects a longitudinal gradient whose fluvial-peripheral dynamics maintain low-medium values, while lake areas maintain higher values. The reclassification, which contains seven levels, summarizes the relative risk by showing sites that fall into suboptimal ranges above or close to thermal maximums, representing areas that are more vulnerable to warming episodes and synergistic effects on water quality.

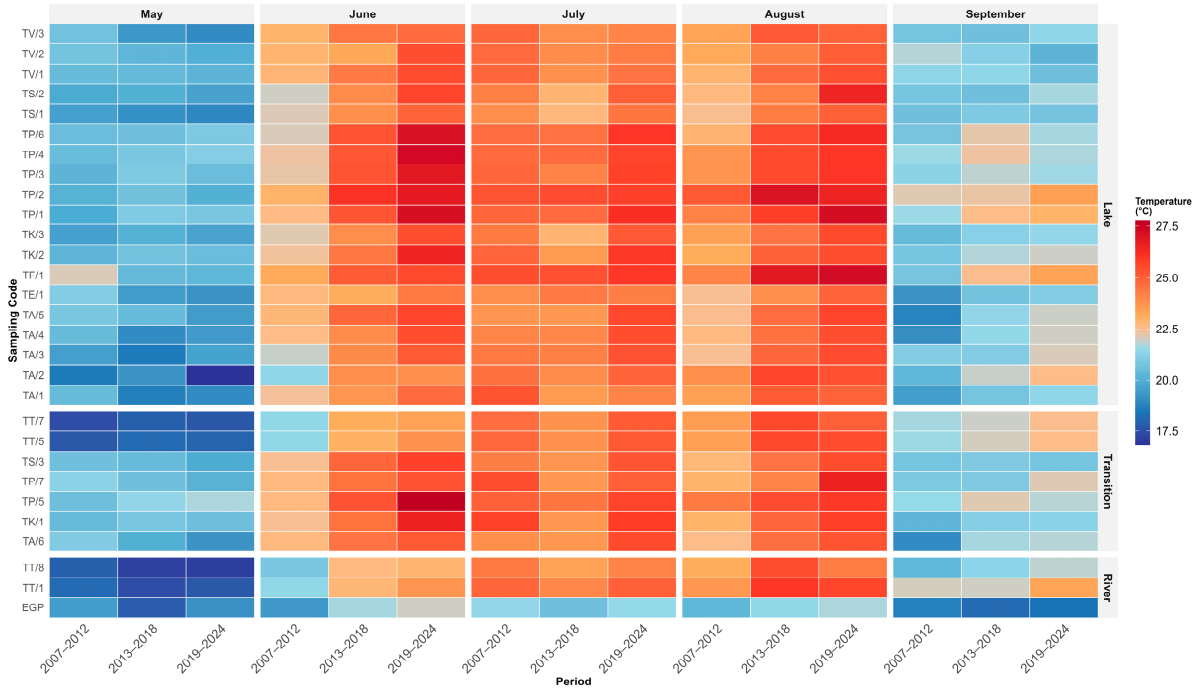


Figure 2. Temperature dynamics across lake–transition–river zones (2007–2024).

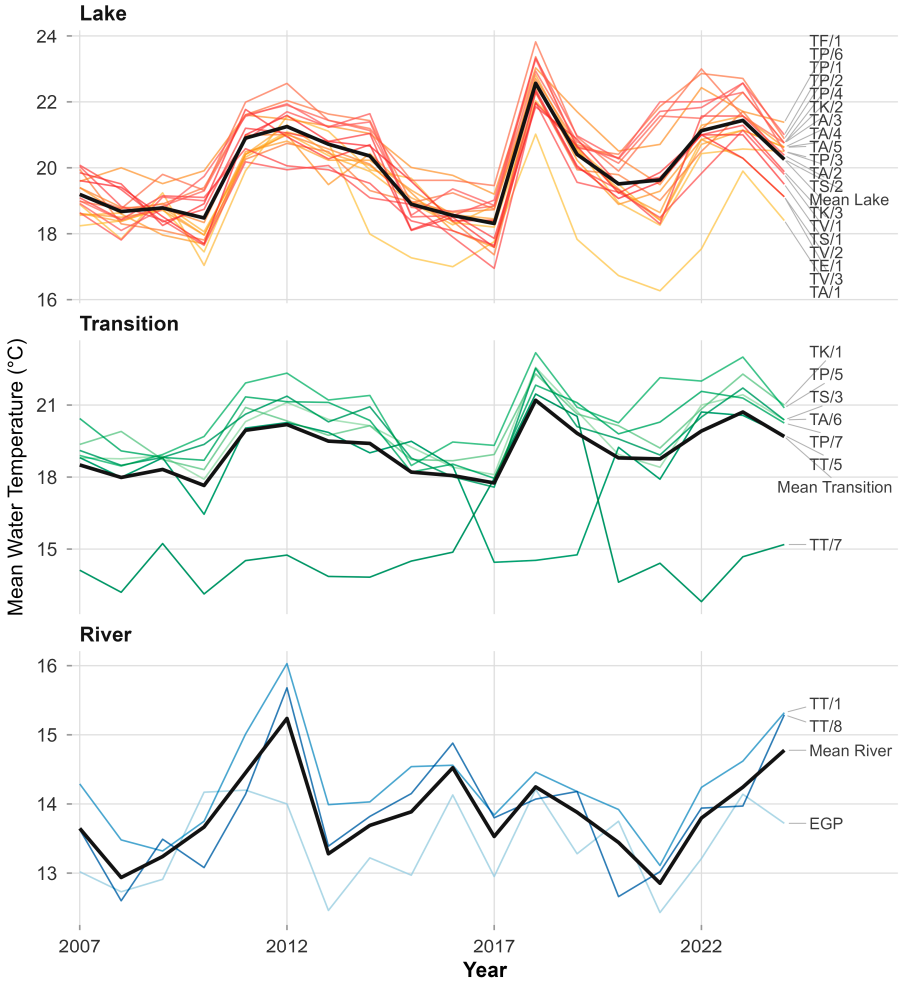


Figure 3. Temporal evolution of the average annual temperature (°C) from May to September by site and category.

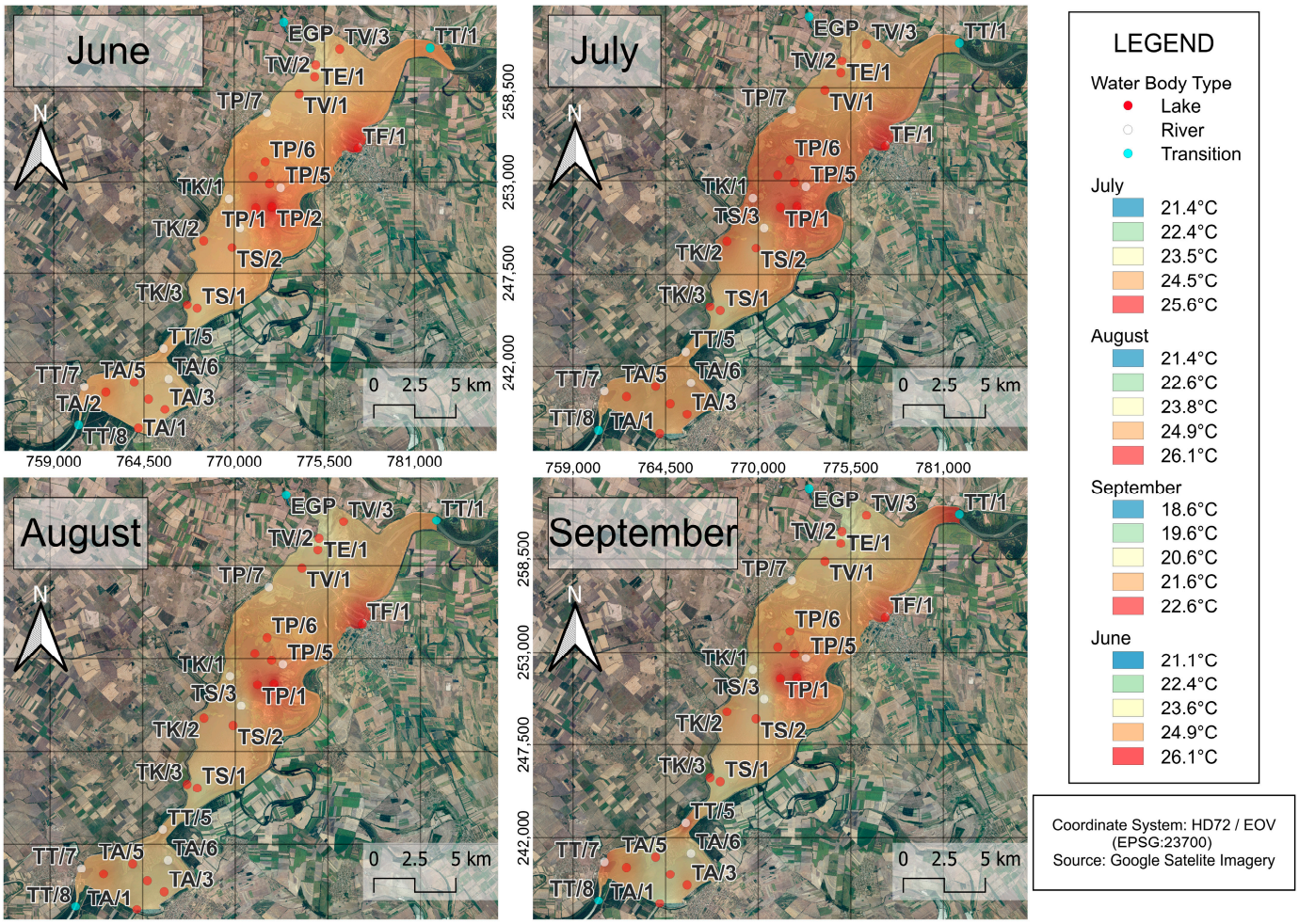


Figure 4. Average surface temperature (2007–2024) for June to September.

3.2. Statistical Evaluation of Thermal Trends (2007–2024)

The proportion of years classified as thermally critical increased consistently across the three monitoring periods and in all hydrological regimes (Figure 6). Thermally critical years were defined as those classified either as class 1, corresponding to Critical Thermal Minimum, or class 7, corresponding to Critical Thermal Maximum. In river stations, the proportion of critical years increased from 22.2% in G1 (2007–2012) to 44.4% in G2 (2013–2018) and 57.1% in G3 (2019–2024). Transitional stations showed a similar increase, from 21.4% to 35.7% and finally to 55.6%. The most pronounced pattern was observed in lake stations, where thermally critical years increased from 59.6% in G1 to 66.7% in G2 and reached 90.4% in G3. This trend is consistent with the spatial patterns shown in Figures 4 and 5, where lacustrine areas exhibited the highest and most persistent thermal values. Overall, the results indicate a clear intensification of thermal stress following the gradient lake > transition > river.

In line with the annual temperature trend (2007–2024) (Figure 7), there is a marked growing pattern, with gradual increases consistent with the accumulation of heat previously in the three hydrological regimes, but underlying the increase throughout the lake system following a direct connection with critical years. Although the analysis is not a predictive model, it suggests that the gradual increase will tend to rise successively, meaning that stress thresholds will become more common.

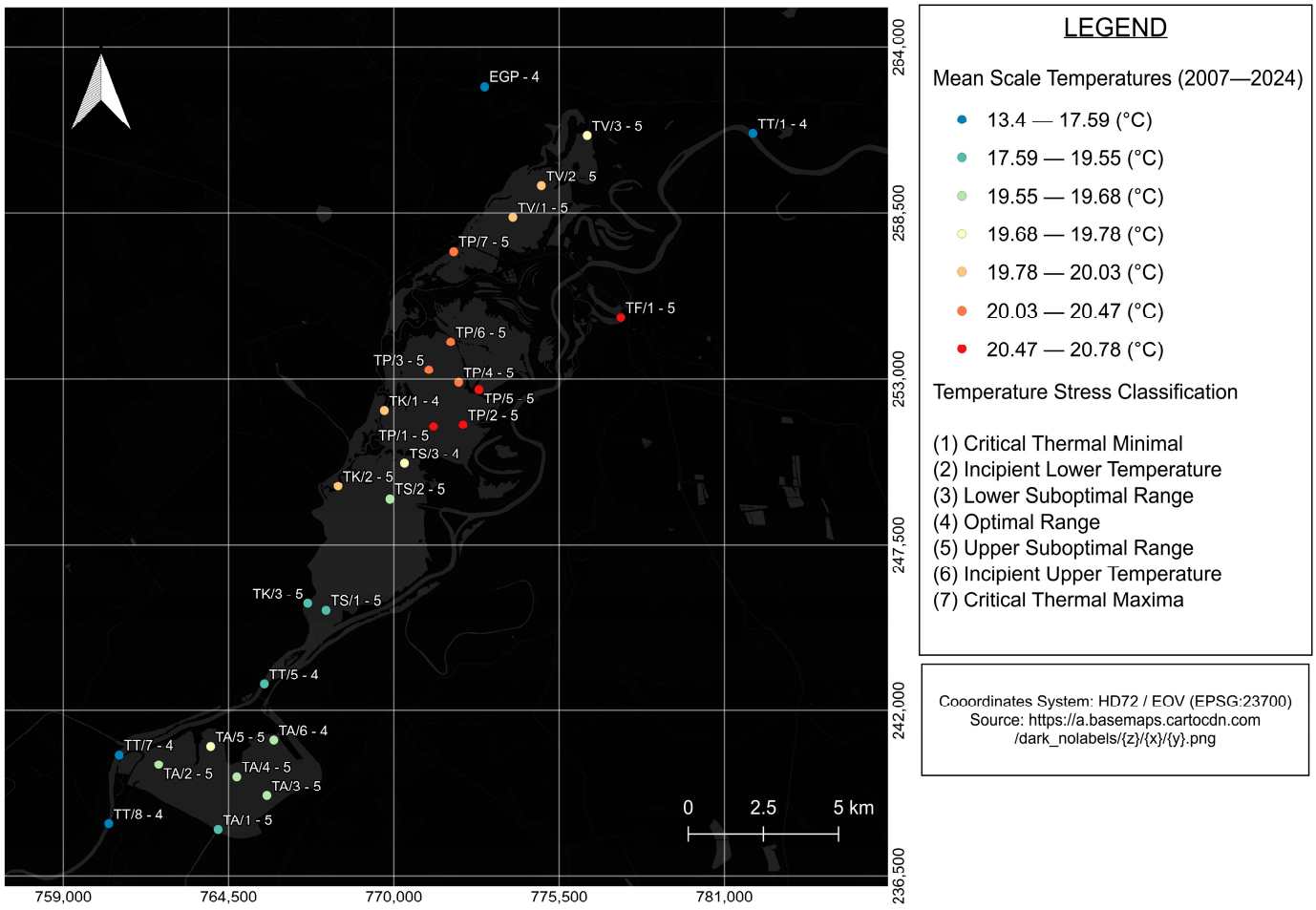


Figure 5. Heat stress index based on mean temperature.

The thermal distribution (Figure 8) confirms that the river, the transition zone, and the lake have their own hierarchical thermal regimes. The river acts as a thermally buffered system (with low temperatures and little variability), while the transition zone and the lake behave as accumulator systems (with more heat and greater heterogeneity). The lake shows a shift towards higher temperatures with a marked right tail, indicating persistent thermal hotspots. The outliers also reveal that extreme weather events occasionally modulate this structural regime.

The trend analysis reveals a robust differential and asymmetric pattern for maximum temperatures and high dispersion, slopes close to zero, and negative values for minimum temperatures (Figure 9). However, the model that works with average temperatures shows an increase, indicating that warming operates on central values, which contributes to the probability of exceeding summer stress thresholds at the ecological level, maintaining an increase, as seen in Table 4.

Table 4. Average regression coefficient by type.

Water Type	Trend, °C/Decade–°C/Year
River	0.2429 °C/decade–0.0243 °C/year
Transition	0.8718 °C/decade–0.0872 °C/year
Lake	0.897 °C/decade–0.0898 °C/year

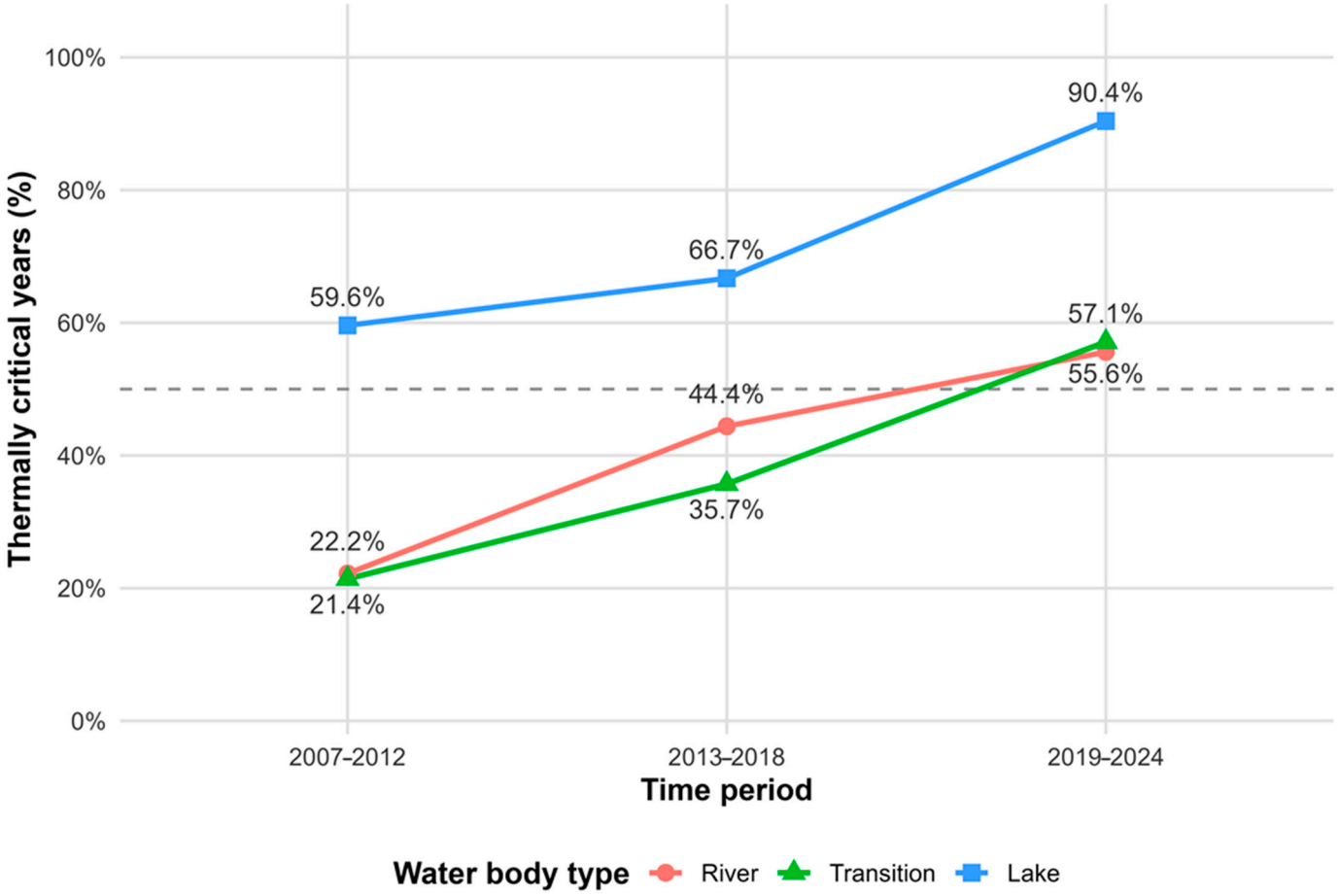


Figure 6. Critical thermal-year proportions across time periods classified as critical (class 1 or 7).

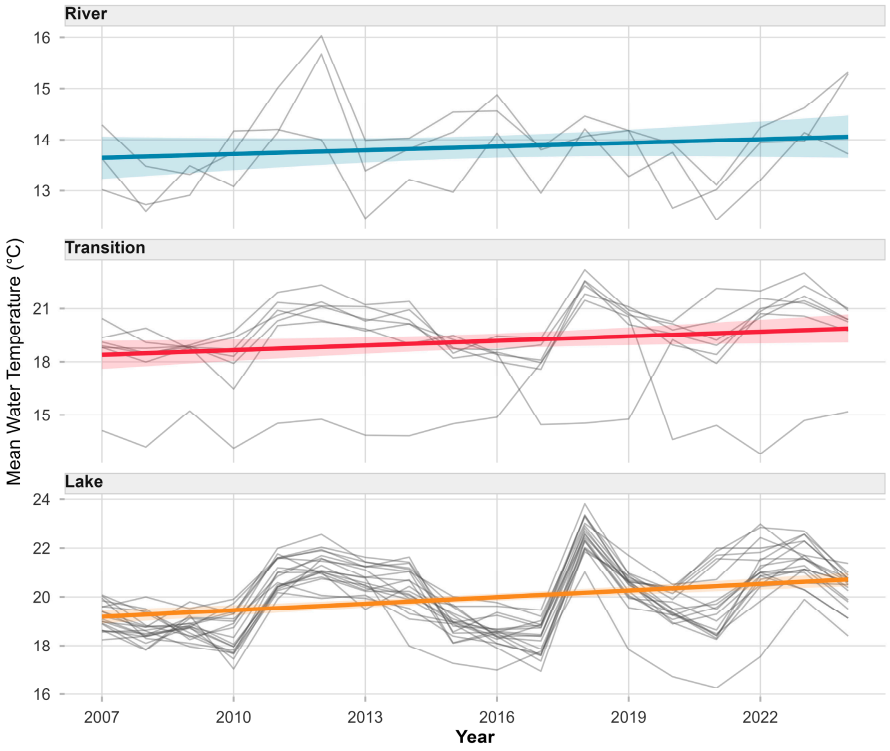


Figure 7. Annual trend of mean water temperature (2007–2024) by hydrological regime.

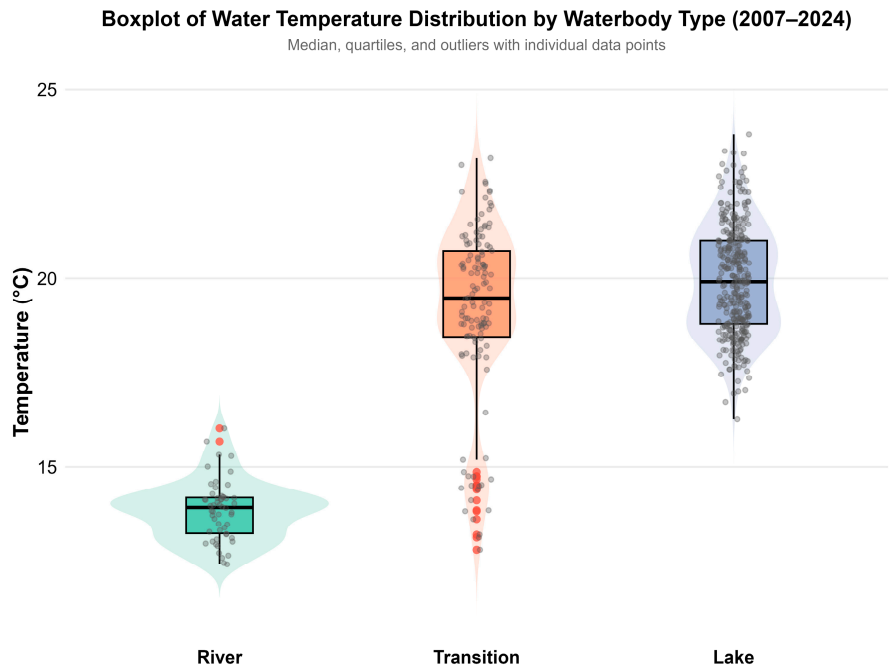


Figure 8. Comparison of all records by category (median/IQR/outliers).

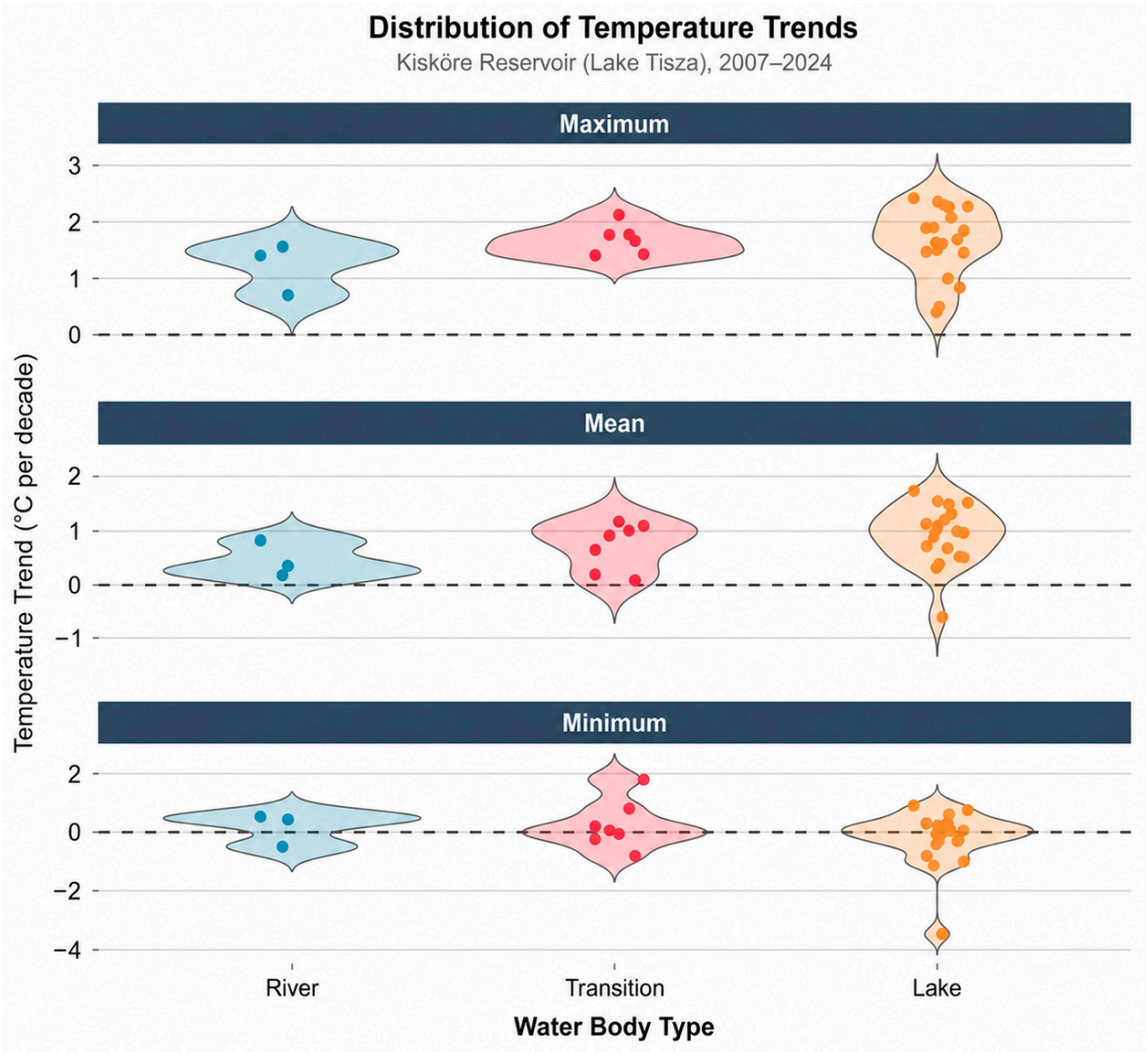


Figure 9. Simple linear model of metric °C/decade distribution.

3.3. Lake Tisza Dissolved Oxygen Summary (2007–2024)

Dissolved oxygen concentrations were closely linked to the thermal regime of the reservoir. Mean values across Lake Tisza generally ranged from 8.0 to 9.6 mg/L, suggesting overall acceptable oxygenation. Nevertheless, localized decreases were observed in the Tiszavalk area, where mean concentrations dropped to approximately 6.8–7.6 mg/L. These lower values may indicate increased oxygen demand, limited hydraulic renewal, or longer residence time, conditions that can enhance ecological sensitivity under warming. When interpreted together with the spatial temperature patterns, these zones coincide with areas of increased vulnerability to oxygen depletion and potential hypoxic stress.

In turn, the monitoring points are characterized under the classification established in Table 2 for dissolved oxygen, maintaining category 3 for the average (Figure 10). The label for each monitoring site indicates the site code, dissolved oxygen concentration in mg/L (2007–2024), and category (1–5).

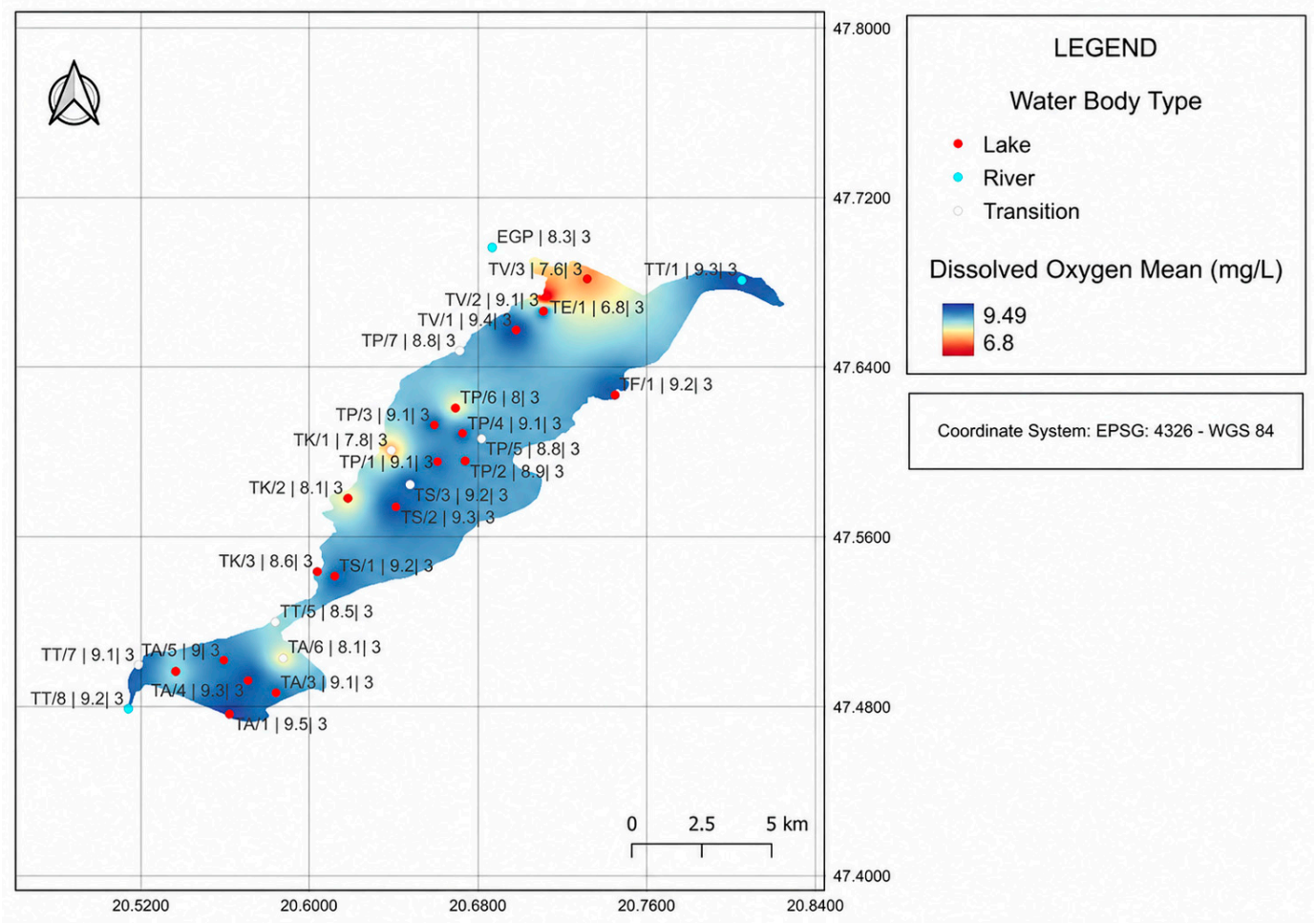


Figure 10. Lake Tisza dissolved oxygen summary (2007–2024): mean.

The Shapiro–Wilk test confirmed non-normal distributions for all groups ($p < 0.001$), justifying the use of Spearman's rank correlation. A 95% confidence interval linear model was fitted to visualize the relationship (Figure 11). The resulting Spearman's ρ was strongest in the river ($\rho = -0.83$), where physical control (oxygen solubility and turbulent mixing) dominates, weakening in the transition zone ($\rho = -0.65$) and further in the lake ($\rho = -0.53$), where biochemical oxygen demand and internal processes introduce additional variability.

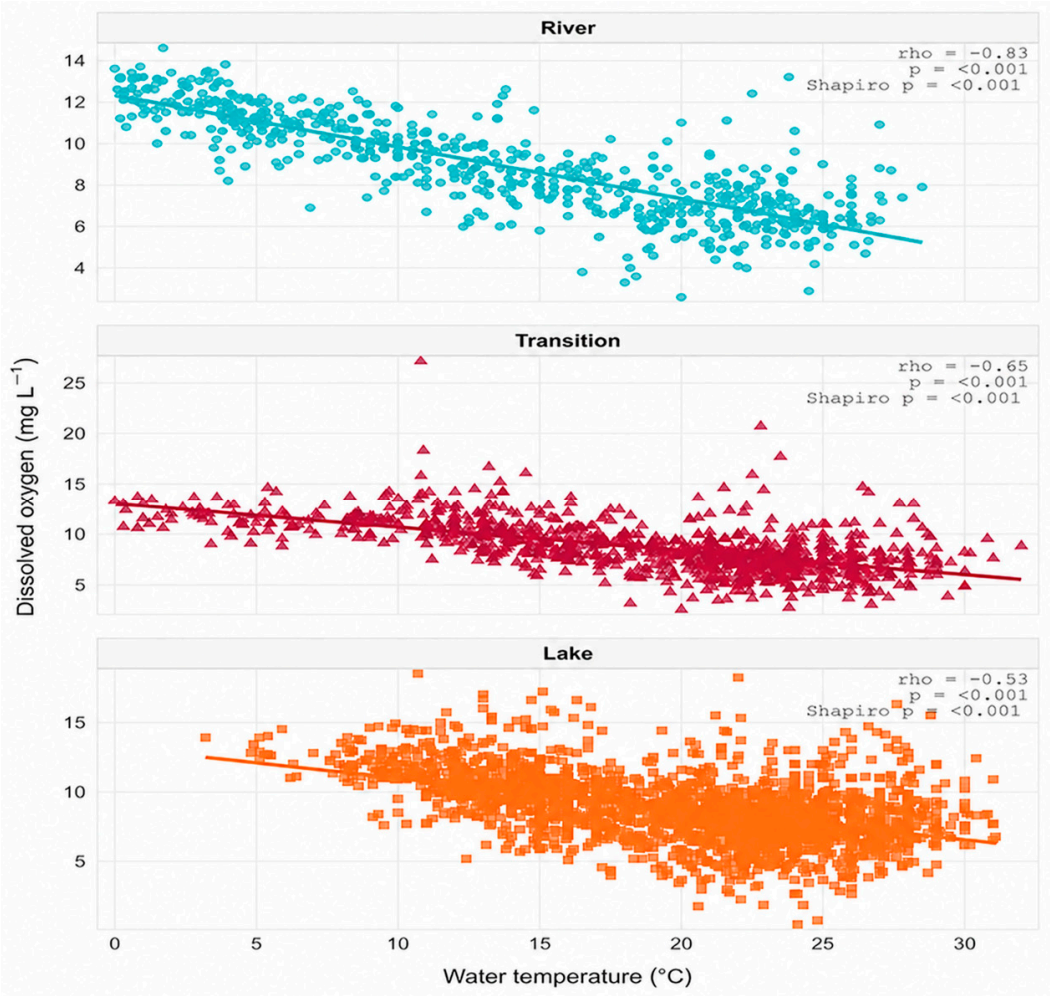


Figure 11. Temperature–dissolved oxygen relationship for waterbody type by the Shapiro–Wilk correlation method; linear model 95% confidence.

3.4. Water Quality Index (WQI) Distribution by Ecosystem Type

The Water Quality Index (WQI) (Figure 12) density distribution reveals a trajectory of improvement from period G1 (2007–2012), G2 (2013–2018) and G3 (2019–2024) in the three types of ecosystems, reflecting a relative reduction in the combined pressure exerted by the physicochemical and microbiological parameters (conductivity, pH, BOD, nitrogen, phosphorus, total coliforms). The improvement is based on mixing processes, dilution, hydraulic renewal, wide internal spatial distribution, or strong hydrological control with a constant flow of water.

The improvement in WQI suggests that the effects associated with these parameters have decreased overall (eutrophication–organic pollution), offsetting the effects of warming. However, the fact that the values are still below 80 means that there is a probability of episodes where critical parameters limit quality. Nevertheless, there is a growing vulnerability due to temperature.

3.5. Multivariate Spatial Organization Analysis of Water Quality Gradients

3.5.1. Principal Component Analysis (PCA) in Transition–River–Lake Systems

Principal component analysis (PCA) was performed on the data from each monitoring period (G1: 2007–2012; G2: 2013–2018; G3: 2019–2024) in order to evaluate the spatial organization of the conventional water quality conditions. This was based on period averages for each station of the six variables included in the conventional WQI: electrical conductivity, pH, BOD_5, total nitrogen, total phosphorus and total coliforms. Temperature

and dissolved oxygen were not included in the PCA as they were evaluated independently as thermal–oxygen stress indicators. (Figure 13).

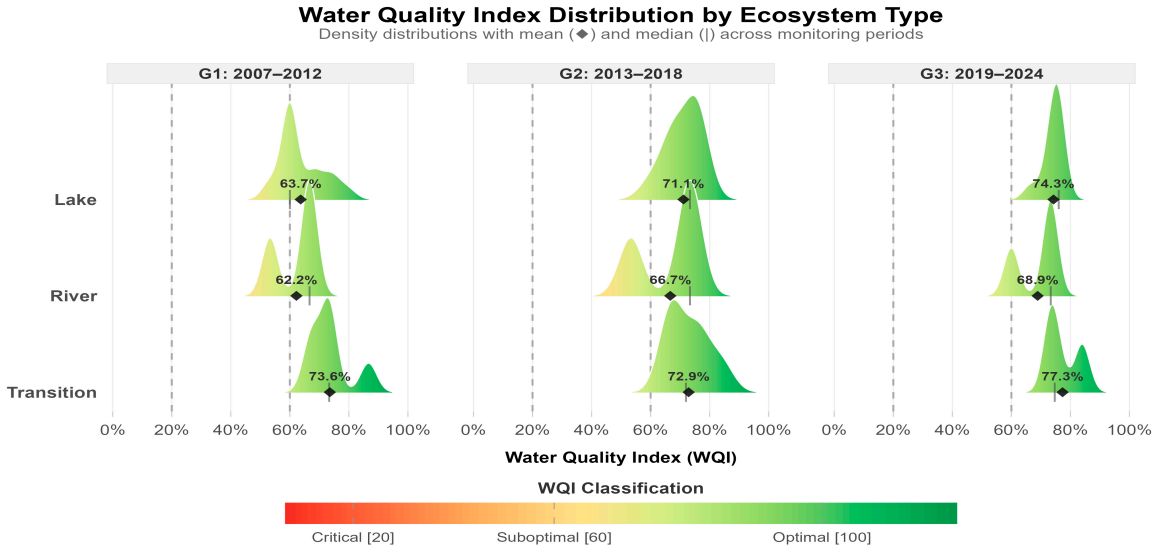


Figure 12. WQI distribution by type and monitoring period, calculated from conductivity, pH, BOD5, total nitrogen, total phosphorus, and total coliforms.

For G1 (2007–2012), the PCA showed 84.7% of the total variance, a clear separation among monitoring sites along the first two principal components, reflecting spatial differences in nutrient enrichment, organic pollution, and microbiological pressure. The main gradient was associated with conductivity, total nitrogen, total phosphorus, BOD5, and coliforms, indicating the influence of eutrophication and organic matter inputs (Figure 13).

For G2 (2013–2018), PC1 and PC2 explained 86.4% of the total variance (PC1 = 64.7%; PC2 = 21.7%) and the ordination pattern suggested a partial reorganization of the monitoring sites. Lake and transition sites showed greater overlap, indicating more homogeneous environmental conditions during this period. The PCA loadings also suggested that nutrient-related and organic pollution variables continued to structure the main environmental gradient.

For G3 (2019–2024), the PCA indicated 85.2%. A stronger spatial convergence was found among several lake and transition sites, while some river-related sites remained differentiated. This pattern suggests that recent environmental conditions may have reduced part of the spatial heterogeneity observed in previous periods, although nutrient enrichment and organic pollution gradients remained relevant (Figure 13).

3.5.2. Hierarchical Clustering Dendrograms (Ward's Method and Euclidean Distance)

The results of the HCA are presented in Table 5, which summarizes the principal clusters identified for each investigated period. The clustering dendrograms indicate a clear spatial differentiation among the monitoring sites, with river, transition and lacustrine groups forming distinct clusters throughout the investigated period (Figure 14). The river sites were generally characterized by more favourable oxygen conditions and lower organic and nutrient loads, whereas the lacustrine sites showed stronger signs of water quality degradation, particularly in relation to organic matter, nutrient enrichment and coliform contamination.

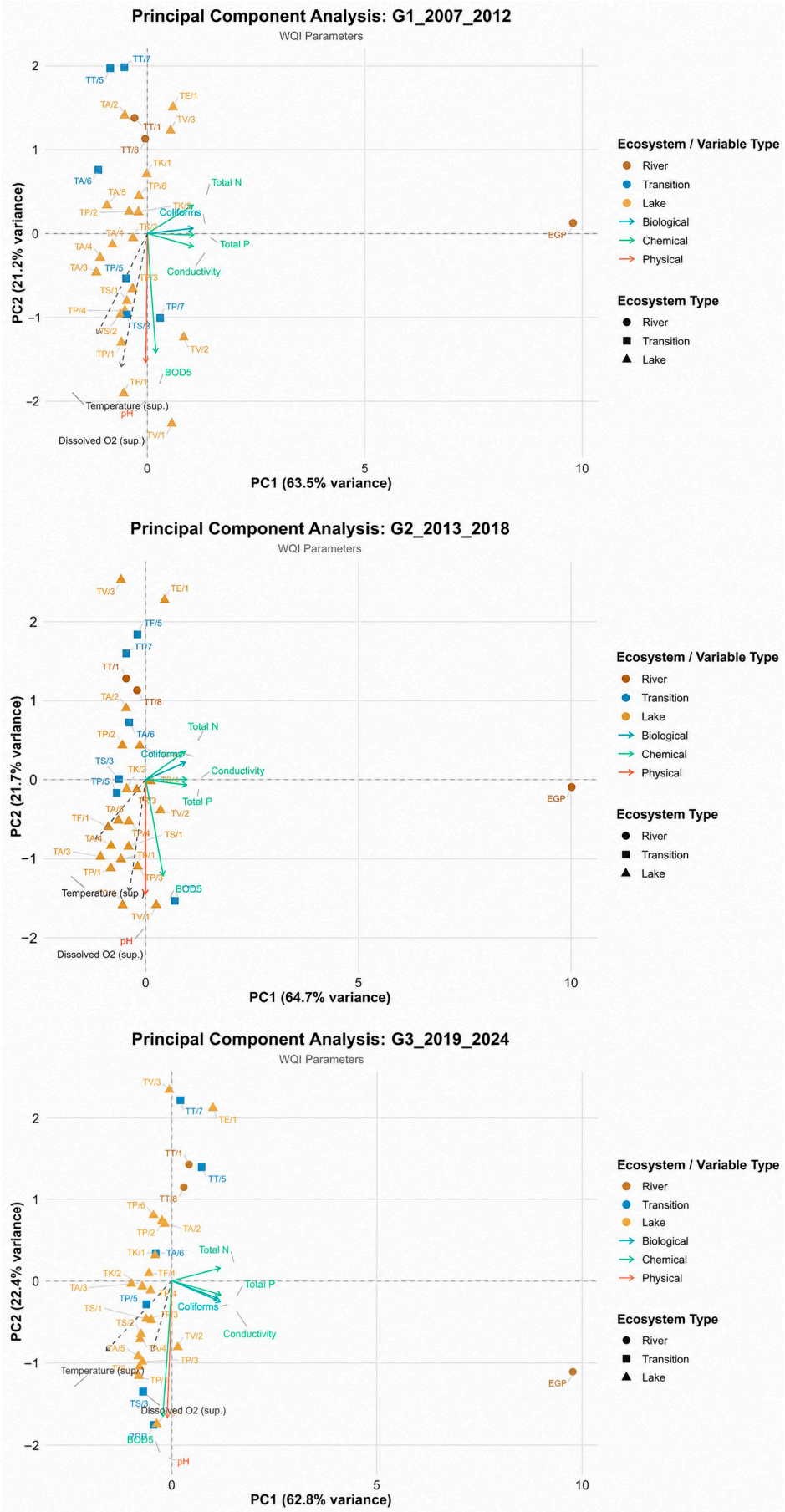
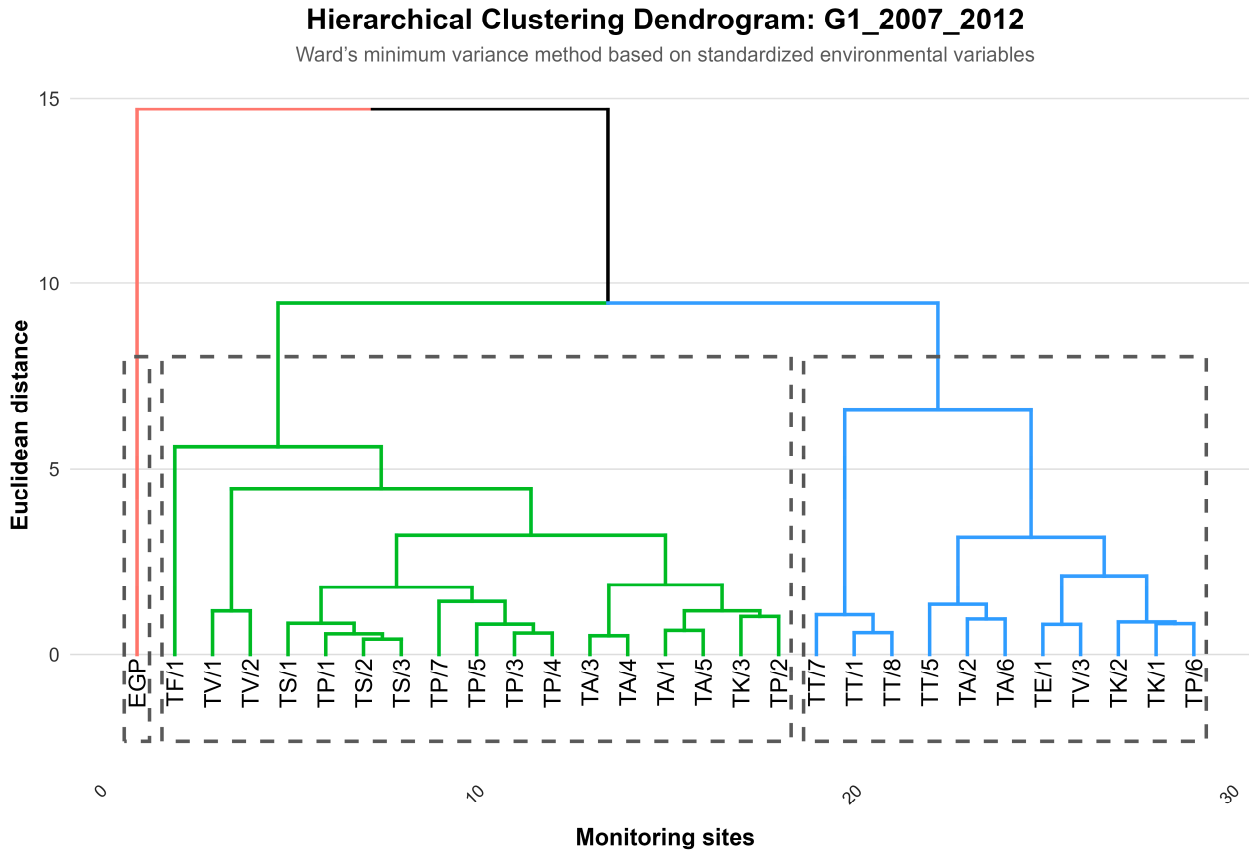


Figure 13. PCA: period G1–period G2–period G3.



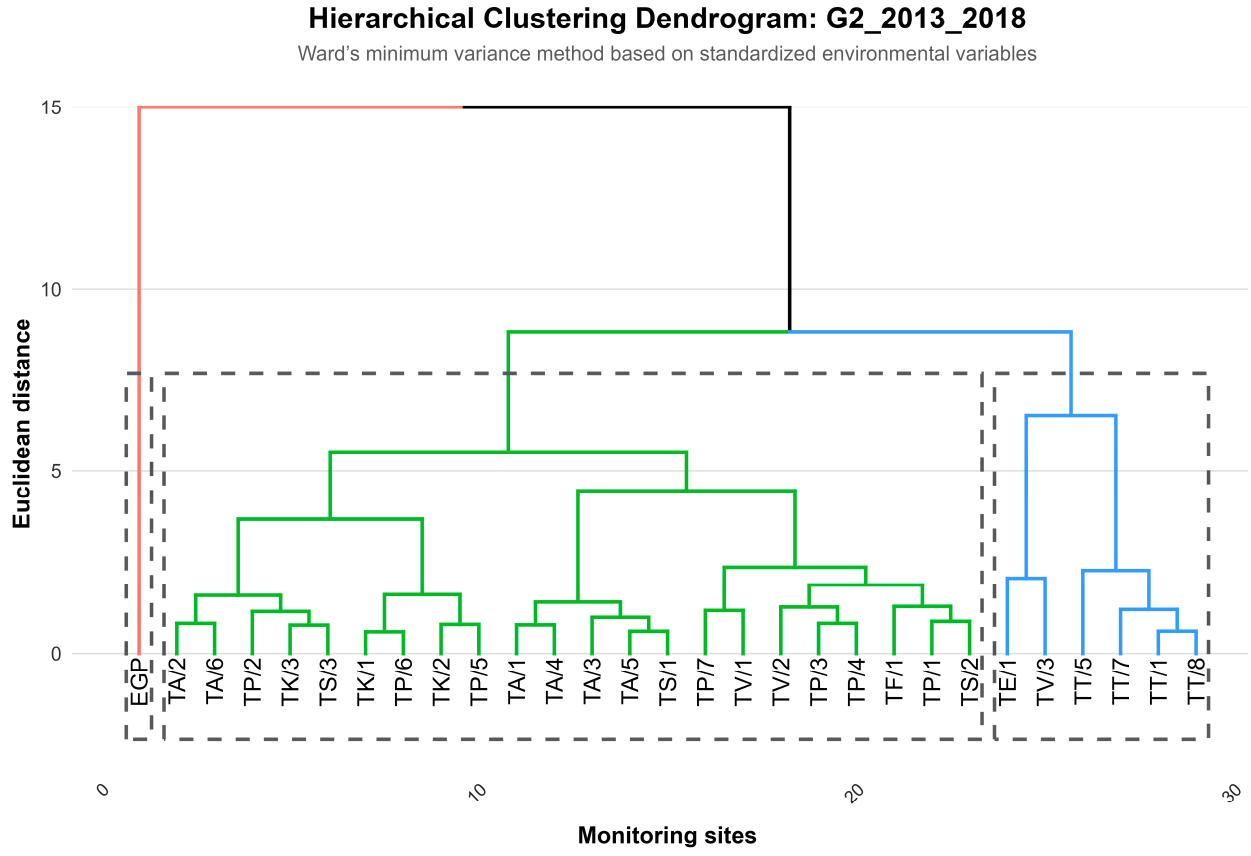


Figure 14. *Cont.*

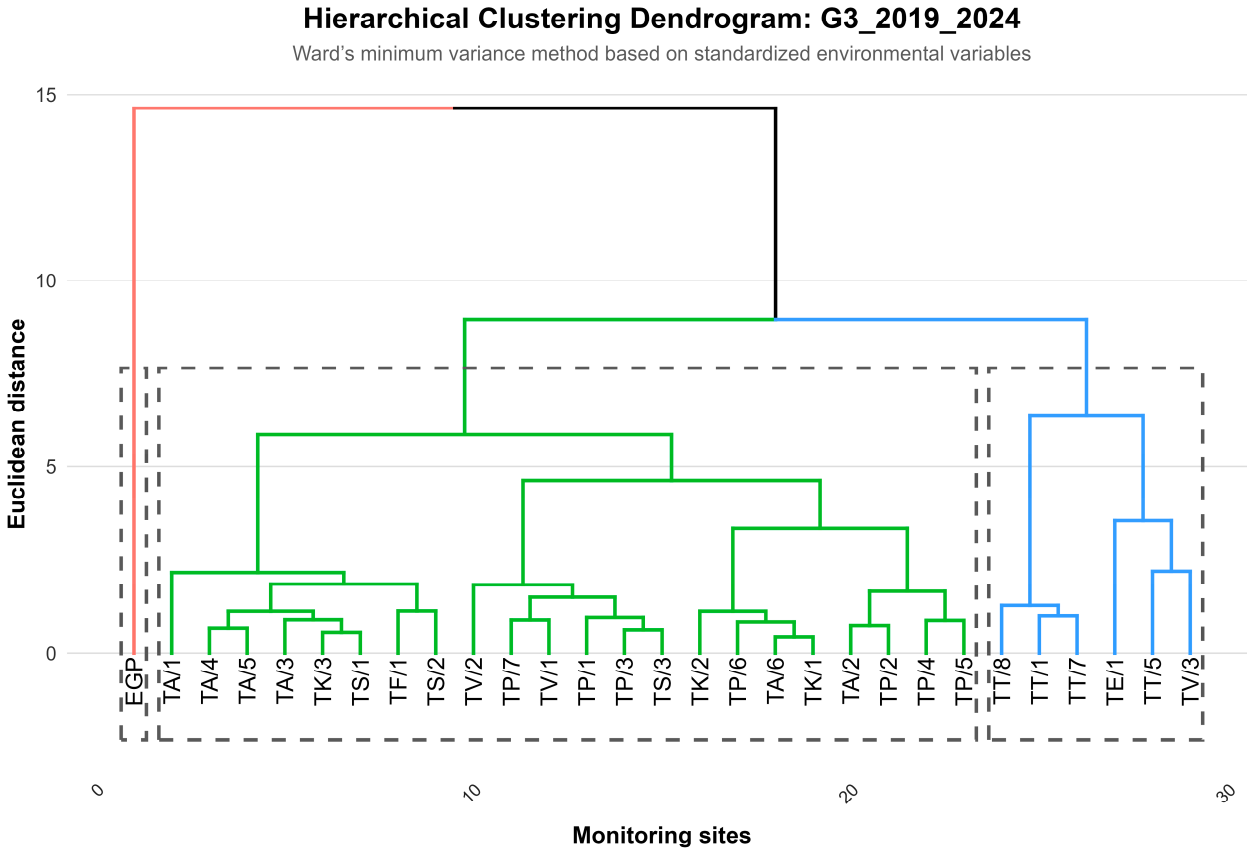


Figure 14. Hierarchical distribution dendrograms by type.

Table 5. General interpretation of the clustering per period.

Periods	Principal Clusters	
2007–2012	River Cluster	Groups sites such as transition and river, denoting better oxygenated conditions and lower organic load (Figure 14)
	Transition Cluster	Integrates transition zones and lake with moderate eutrophication and increasing internal similarity
	Lacustrine Cluster	More dispersed, it integrates sites with impact, high BOD, nutrients, and coliforms, evidencing eutrophication and a low Water Quality Index (63–74), denoting marginal conditions in lake ecosystems
2013–2018	River Cluster	It shows greater compaction/homogeneity with some signs of improved quality (Figure 14)
	Transition Cluster	It suggests a relative improvement in transition zones and lakes, reciprocal with the increase in WQI in ecotones of 77.3
	Lacustrine Cluster	It has a broader and more subdivided structure due to coliforms as a differentiating variable, the lake remaining the most impacted site
2019–2024	River Cluster	It is the most homogeneous and separate group, with high oxygenation and low coliform load (Figure 14)
	Transition Cluster	It reflects a reduction in BOD and nutrients, linking transitions to moderate lakes
	Lacustrine Cluster	It persists with impacted sites, has defined subgroups and less heterogeneity, confirming an improvement associated with coliforms and nutrients

4. Discussion

Highly relevant information regarding freshwater ecosystems indicates that the main cause of degradation is the increase in temperature captured from the atmosphere and exacerbated during summer periods. Global surface water warming documented over the past 150 years in the Pannonian Ecoregion shows an average rate of 0.317 °C/decade across lakes and rivers combined [31], with the majority of this warming concentrated in the last three to four decades. At the global scale, lake summer surface temperatures warmed at a mean rate of 0.34 °C/decade between 1985 and 2009, with individual lakes reaching up to 0.72 °C/decade depending on local climatic and morphometric conditions [7]. The warming rate detected in this study for Lake Tisza (0.90 °C/decade in lacustrine zones, 2007–2024) substantially exceeds both the Pannonian regional average [31] and the global benchmark [7], reinforcing the particular thermal vulnerability of shallow, low-residence-time reservoirs under accelerating climate forcing.

These phenomena are closely related to summer thermal stress, which can increase the probability of algal blooms and hypoxia, particularly in shallow and hydrologically less dynamic areas [9]. The hierarchical clustering results also indicate a partial homogenization of monitoring sites, suggesting reduced spatial variability in water quality conditions during the most recent period. This interpretation is supported by the PCA, where the dominant gradients were mainly associated with nutrient enrichment, organic matter inputs, conductivity, and microbiological contamination. However, the observed improvement in coliform-related scores indicates that microbiological conditions improved at several sites, even though thermal and nutrient-related pressures continued to influence the overall ecological status [32].

The quality index shows a change in marginal conditions from 63.7 to high suboptimal conditions of 74.3. In G3, there was a transition from 73.6 to 77.3 (approaching optimal), with rivers stabilizing around 62.2–68.9, indicating an improvement in ecosystem services related to tourism [3]. The transitions suggest resilience, probably due to the reduction in fecal contamination.

This, in turn, is due to adaptive measures such as the restoration of floodplains and water retention measures in the middle Tisza [33,34]. Showing peak flows and reducing the amount of nutrients and organic matter during high discharge events, this mechanism directly reduces BOD_5 loading and total nitrogen and phosphorus inputs as the main driver of eutrophication, as reflected in the WQI improvement from G1 to G3. Water retention measures extend hydrological residence time in adjacent agricultural areas, promoting sedimentation of suspended solids and denitrification in riparian zones before water reaches the lake [33,35,36]. Hydrological interventions, such as regulated water-level management in the reservoir, also improve vertical mixing and oxygenation, counteracting thermal stratification, a process particularly relevant in the shallow lake sector (mean depth 1.45 m) where stratification risk increases with warming [3]. Together, these nature-based solutions do not address the thermal component directly, but mitigate the compounding biochemical consequences of warming, explaining why conventional water quality indicators show improvement even as temperature indicators deteriorate [3,33]. Hydrological interventions mitigate effects such as eutrophication and stratification, among other potential harmful effects on the environment [32].

This study's approach to climate change is still limited by the absence of certain physicochemical or biological parameters (macroinvertebrates, phytoplankton) that could refine the level of eutrophication, meaning that some critical points are overlooked in the current draft of the article. Changes in land use deserve attention in terms of how to integrate them into a model for greater accuracy. The current temperature model reveals asymmetry and a clear response to the advances of climate change with a discouraging trend. Therefore,

a future orientation towards 50-year predictive models should combine hydrodynamic models vs. heat waves [31], solutions on how to increase their resilience [33], analysis of stress factors such as salinization [37], and the thermotolerance of the area's ichthyofauna, considering that it is a tourist and recreational area which depends economically in part on tourist activity [3]. Even more so, this could be achieved by raising awareness and expanding knowledge, thus ensuring the viability of the Tisza system in a context of rapid change.

5. Conclusions

In the present study, the progressive thermal intensification experienced by Lake Tisza between 2007 and 2024 is characterized by a more frequent exacerbation of temperature with a more constant pattern throughout the three water flows, with the lake being the most vulnerable. The inversely proportional relationship between temperature and dissolved oxygen confirms the pressure on the functioning of the system. At the same time, the water quality index (WQI), which integrates conductivity, pH, biological oxygen demand (BOD), nitrogen, phosphorus, and coliforms, reflected a relative progressive improvement in the different periods, showing a nonlinear ecosystem dynamic coexisting with an increasing thermal risk. Multivariate spatial analyses (WQI, trend assessment, clustering, PCA) indicate a complex environmental reorganization shaped by climate, hydrodynamics, and reservoir heterogeneity, rather than simple degradation or recovery. This highlights the need to implement more robust monitoring frameworks in terms of physical–chemical parameters that cover thermal vulnerability, thus obtaining an assessment that reflects the reality of the ecological resilience of this system.

Supplementary Materials: The following supporting information can be downloaded at: https://www.mdpi.com/article/10.3390/w18111365/s1, Supplementary S1: Detailed description of statistical methods.

Author Contributions: Conceptualization. D.M. and T.M.; methodology. D.M., T.M. and E.C.; software. G.S. and D.M.; validation. T.M. and E.K.; formal analysis. D.M., T.M. and G.S.; investigation. B.B., E.C. and M.V.; resources. T.M., P.C. and G.S.; data curation. E.C. and G.S.; writing—original draft preparation. D.M. and T.M.; writing—review and editing. T.M., G.S., E.K. and P.C.; visualization. D.M.; supervision. T.M. All authors have read and agreed to the published version of the manuscript.

Funding: Project no. TKP2021-NKTA-32 has been implemented with the support provided from the National Research Development and Innovation Fund of Hungary. Financed under the TKP2021-NKTA funding scheme. Supported by the University of Debrecen Scientific Research Bridging Fund (DETKA).

Data Availability Statement: The data presented in this study are available on request from the corresponding author due to restrictions imposed by the data provider. According to the data management policy of the Middle Tisza District Water Directorate, the disclosure or sharing of the dataset requires the Directorate's prior approval.

Acknowledgments: We acknowledge the assistance provided by the Middle Tisza District Water Directorate in providing the results of laboratory measurements.

Conflicts of Interest: The authors declare no conflicts of interest.

Abbreviations

The following abbreviations are used in this manuscript:

PCA	Principal Component Analysis
WQI	Water Quality Index
IPCC	Intergovernmental Panel on Climate Change
IQR	Interquartile Range

References

1. Caretta, M.A.; Mukherji, A.; Arfanuzzaman, M.; Betts, R.A.; Gelfan, A.; Hirabayashi, Y.; Lissner, T.K.; Liu, J.; Lopez Gunn, E.; Morgan, R.; et al. Water. In *Climate Change 2022—Impacts, Adaptation and Vulnerability*; Cambridge University Press: Cambridge, UK, 2023; pp. 551–712.
2. Vári, Á.; Podschun, S.A.; Erős, T.; Hein, T.; Pataki, B.; Iojă, I.-C.; Adamescu, C.M.; Gerhardt, A.; Gruber, T.; Dedić, A.; et al. Freshwater Systems and Ecosystem Services: Challenges and Chances for Cross-Fertilization of Disciplines. *Ambio* **2022**, *51*, 135–151. [CrossRef] [PubMed]
3. Mester, T.; Benkhard, B.; Vasvári, M.; Csorba, P.; Kiss, E.; Balla, D.; Fazekas, I.; Csépes, E.; Barkat, A.; Szabó, G. Hydrochemical Assessment of the Kisköre Reservoir (Lake Tisza) and the Impacts of Water Quality on Tourism Development. *Water* **2023**, *15*, 1514. [CrossRef]
4. Paerl, H.; Otten, T. Harmful Cyanobacterial Blooms: Causes, Consequences, and Controls. *Microb. Ecol.* **2013**, *65*, 995–1010. [CrossRef]
5. Amorim, C.A.; do Nascimento Moura, A. Ecological Impacts of Freshwater Algal Blooms on Water Quality, Plankton Biodiversity, Structure, and Ecosystem Functioning. *Sci. Total Environ.* **2021**, *758*, 143605. [CrossRef]
6. Parmesan, C.; Morecroft, M.; Trisurat, Y. Terrestrial and Freshwater Ecosystems and Their Services. In *Climate Change 2022—Impacts, Adaptation and Vulnerability*; Cambridge University Press: Cambridge, UK, 2023; pp. 197–378.
7. O'Reilly, C.M.; Sharma, S.; Gray, D.K.; Hampton, S.E.; Read, J.S.; Rowley, R.J.; Schneider, P.; Lenters, J.D.; McIntyre, P.B.; Kraemer, B.M.; et al. Rapid and Highly Variable Warming of Lake Surface Waters around the Globe. *Geophys. Res. Lett.* **2015**, *42*, 10773–10781. [CrossRef]
8. Woolway, R.I.; Merchant, C.J. Worldwide Alteration of Lake Mixing Regimes in Response to Climate Change. *Nat. Geosci.* **2019**, *12*, 271–276. [CrossRef]
9. Jane, S.; Hansen, G.; Kraemer, B.; Leavitt, P.; Mincer, J.; North, R.; Pilla, R.; Stetler, J.; Williamson, C.; Woolway, R.; et al. Widespread Deoxygenation of Temperate Lakes. *Nature* **2021**, *594*, 66–70. [CrossRef]
10. Paerl, H.W.; Huisman, J. Climate Change: A Catalyst for Global Expansion of Harmful Cyanobacterial Blooms. *Environ. Microbiol. Rep.* **2009**, *1*, 27–37. [CrossRef] [PubMed]
11. Rodgers, E.M. Adding Climate Change to the Mix: Responses of Aquatic Ectotherms to the Combined Effects of Eutrophication and Warming. *Biol. Lett.* **2021**, *17*, 20210442. [CrossRef] [PubMed]
12. Meyer-Jacob, C.; Michelutti, N.; Paterson, A.M.; Cumming, B.F.; Keller, W.; Smol, J.P. The Browning and Re-Browning of Lakes: Divergent Lake-Water Organic Carbon Trends Linked to Acid Deposition and Climate Change. *Sci. Rep.* **2019**, *9*, 16676. [CrossRef] [PubMed]
13. Herreid, A.M.; Fazekas, H.M.; Nelson, S.J.; Wymore, A.S.; Murray, D.; Varner, R.K.; McDowell, W.H. Climate Displaces Deposition as Dominant Driver of Dissolved Organic Carbon Concentrations in Historically Acidified Lakes. *Biogeochemistry* **2024**, *168*, 5. [CrossRef] [PubMed]
14. Poff, N.L.; Zimmerman, J.K.H. Ecological Responses to Altered Flow Regimes: A Literature Review to Inform the Science and Management of Environmental Flows. *Freshw. Biol.* **2010**, *55*, 194–205. [CrossRef]
15. ICPDR. *Updated Integrated Tisza River Basin Management Plan*; ICPDR: Vienna, Austria, 2019.
16. The European Parliament and the Council of the European Union. *Diario Oficial de Las Comunidades Europeas ES*; The European Parliament and the Council of the European Union: Strasbourg, France, 2000.
17. Znachor, P.; Kosour, D.; Rederer, L.; Koza, V.; Kolář, V.; Nedoma, J. Tracking Reservoir Warming in a Changing Climate: A 31-Year Study from Czechia. *Environ. Sci. Ecotechnol.* **2025**, *28*, 100631. [CrossRef]
18. Maberly, S.C.; O'Donnell, R.A.; Woolway, R.I.; Cutler, M.E.J.; Gong, M.; Jones, I.D.; Merchant, C.J.; Miller, C.A.; Politi, E.; Scott, E.M.; et al. Global Lake Thermal Regions Shift under Climate Change. *Nat. Commun.* **2020**, *11*, 1232. [CrossRef]
19. Piccolroaz, S.; Zhu, S.; Ladwig, R.; Carrea, L.; Oliver, S.; Piotrowski, A.P.; Ptak, M.; Shinohara, R.; Sojka, M.; Woolway, R.I.; et al. Lake Water Temperature Modeling in an Era of Climate Change: Data Sources, Models, and Future Prospects. *Rev. Geophys.* **2024**, *62*, e2023RG000816. [CrossRef]
20. Lovász, G. Water Temperatures of the Danube and Tisza Rivers in Hungary. *Hung. Geogr. Bull.* **2012**, *61*, 317–325.
21. Benkhard, B.; Csorba, P.; Mester, T.; Balla, D.; Kiss, E.; Szabó, G.; Fazekas, I.; Vass, R.; Rooien, A.; Vasvári, M. Effects of Mosaic Natural Conditions on the Tourism Management of a Lowland Water Reservoir, Lake Tisza, Hungary. *Land* **2023**, *12*, 2092. [CrossRef]
22. U.S. Geological Survey. Lakes and Reservoirs: Guidelines for Study Design and Sampling. In *Book 9, Handbooks for Water-Resources Investigations*; U.S. Geological Survey: Reston, VA, USA, 2018.
23. Brungs, W.; Jones, B. *Temperature Criteria for Freshwater Fish: Protocol and Procedures*; U.S. Environmental Protection Agency: Washington, DC, USA, 1977.
24. Vidékfejlesztési Minister. *VM Rendelet a Felszíni Víz Vízszennyezettségi Határértékeiről És Azok Alkalmazásának Szabályairól*; Vidékfejlesztési Minister: Budapest, Hungary, 2010.

25. U.S. Environmental Protection Agency. Hypoxia 101. Available online: https://www.epa.gov/ms-htf/hypoxia-101 (accessed on 17 May 2026).
26. Helsel, D.R.; Hirsch, R.M.; Ryberg, K.R.; Archfield, S.A.; Gilroy, E.J. *Tm4a3.Pdf—Statistical Methods in Water Resources*; U.S. Geological Survey: Reston, VA, USA, 2020.
27. Chidiac, S.; Najjar, P.; Ouaini, N.; Rayess, Y.; Azzi, D. A Comprehensive Review of Water Quality Indices (WQIs): History, Models, Attempts and Perspectives. *Rev. Environ. Sci. Biotechnol.* **2023**, *22*, 349–395. [CrossRef]
28. Sutadian, A.D.; Muttil, N.; Yilmaz, A.G.; Perera, B.J.C. Development of River Water Quality Indices—A Review. *Environ. Monit. Assess.* **2016**, *188*, 1–29. [CrossRef]
29. Tyagi, S.; Sharma, B.; Singh, P.; Dobhal, R. Water Quality Assessment in Terms of Water Quality Index. *Am. J. Water Resour.* **2020**, *1*, 34–38. [CrossRef]
30. Dong, Y.; Peng, C.-Y.J. Principled Missing Data Methods for Researchers. *SpringerPlus* **2013**, *2*, 222. [CrossRef] [PubMed]
31. Li, H.; Sun, J.; Zhou, Q.; Sojka, M.; Ptak, M.; Luo, Y.; Wu, S.; Zhu, S.; Tóth, V.R. 150-Year Daily Data (1870–2021) in Lakes and Rivers Reveals Intensifying Surface Water Warming and Heatwaves in the Pannonian Ecoregion (Hungary). *J. Hydrol. Reg. Stud.* **2024**, *56*, 101985. [CrossRef]
32. Takács-György, K.; Nagy-Kovács, Z. Evaluating Climate Change Impacts on Water Safety: A Case Study of the Danube in Budapest. *Ecocycles* **2024**, *10*, 14–25. [CrossRef]
33. Climate-ADAPT. *Temporary Flood Water Storage in Agricultural Areas in the Middle Tisza River Basin—Hungary*; Climate-ADAPT: Copenhagen, Denmark, 2022.
34. Kajner, P.T.; Gruber; Cselószki, T. *Developing Sustainable Water Management and Landscapes in the Tisza Plain. Roadmap to 2050*; European Union's Horizon: Brussels, Belgium, 2024; p. 35.
35. UNDP/GEF. *UNDP/GEF Integrated River Basin Management in the Tisza INCEPTION REPORT Integrating Multiple Benefits of Wetlands and Floodplains into Improved Transboundary Management for the Tisza River Basin*; UNDP/GEF: Washington, DC, USA, 2008.
36. LIFE SUMAR. *Theme: The Overall Context of Agriculture and Nature Conservation*; LIFE SUMAR: Szolnok, Hungary, 2007.
37. Radosavljevic, J.; Shahvaran, A.; Van Cappellen, P. *Beyond Climate Warming: How Salinization Accelerates Deoxygenation in Lakes*; Federated Research Data Repository: Waterloo, ON, Canada, 2025.

Disclaimer/Publisher's Note: The statements, opinions and data contained in all publications are solely those of the individual author(s) and contributor(s) and not of MDPI and/or the editor(s). MDPI and/or the editor(s) disclaim responsibility for any injury to people or property resulting from any ideas, methods, instructions or products referred to in the content.